Trapping of fast magnetoacoustic waves close to an *X* line in a toroidal system

Daniela Farina
Istituto di Fisica del Plasma, Consiglio Nazionale delle Ricerche, EURATOM-ENEA-CNR Association, via Cozzi 53, 20125 Milano, Italy

Roberto Pozzoli
Istituto Nazionale di Fisica delle Materia, Dipartimento di Fisica, Università di Milano, via Celoria 16, 20133 Milano, Italy

(Received 3 July 1996; revised manuscript received 30 October 1996)

The trapping of fast magnetoacoustic waves around the *X* line of a toroidal magnetic configuration is investigated in the framework of ideal magnetohydrodynamics using a WKB approach. The frequency spectrum and the relevant eigenmodes are determined for the hyperbolic case, and for a divertorlike geometry. Striking differences are pointed out, which are due to the breaking of the symmetry in the system. [S1063-651X(97)10605-5]

PACS number(s): 52.35.Bj, 03.65.Sq

I. INTRODUCTION

We refer to a z-periodic magnetic field configuration $\boldsymbol{B}(x,y)=B_z\boldsymbol{e}_z+\boldsymbol{B}_p(x,y)$, with constant B_z and $\boldsymbol{B}_p$ parallel to the (x,y) plane, characterized by a null point of $\boldsymbol{B}_p$, $\boldsymbol{B}_p(0,0)=\boldsymbol{0}$ (X line), and consider ideal magnetohydrodynamic (MHD) perturbations on a uniform, zero β, currentless plasma. This model can be relevant to space plasma, and to laboratory plasma, e.g., the scrape-off layer (SOL) of a divertor configuration in a rectified tokamak geometry.

Analyses of purely two-dimensional (2D) perturbations (i.e., with no z dependence) in similar systems, have been made in Refs. [1,2]. We address here the more general 3D case, and point out the occurrence of new features in the propagation of MHD waves, such as trapping of fast waves around the X line. The determination of the corresponding frequency spectrum, and the related eigenmodes, is the main goal of the present paper. Moreover, we account for the effects of deviations of the poloidal field $\boldsymbol{B}_p$ from the pure hyperbolic configuration usually considered in the literature, and show how they can greatly affect the structure of the modes.

The WKB analysis of fast modes in a current carrying cylindrical system (representing the core of a tokamak plasma) has been performed in Ref. [3]. In the case of the X line, the main difference is the absence of the helical symmetry of the magnetic field lines. We use the WKB approach in the form presented by Littlejohn and Flynn [4], which reduces the problem to the solution of a scalar wave equation, and allows the extension of the analysis to the case of a more general dielectric response. Following the ideal MHD model, we do not consider finite frequency effects, and the problem of linear conversion [5], which will be the subject of a future investigation.

This paper is organized as follows. The basic equations for the WKB solutions are presented in Sec. II. The unperturbed configurations in the hyperbolic and divertorlike cases are introduced in Sec. III. The eigenmode analysis of the fast waves is performed in Sec. IV. Conclusions are given in Sec. V.

II. THE WKB APPROACH

In the framework of the ideal MHD, the equation for a displacement field $\boldsymbol{\xi}(x,y,z)$ with frequency ω is

$$\hat{\mathsf{D}}\boldsymbol{\xi}\equiv 4\pi\rho\omega^2\boldsymbol{\xi}+\boldsymbol{B}\times\{\nabla\times[\nabla\times(\boldsymbol{B}\times\boldsymbol{\xi})]\}=\boldsymbol{0}, \tag{1}$$

where ρ is the constant plasma density, and the operator $\hat{\mathsf{D}}$ is Hermitian.

Within the WKB approach, we introduce a smallness parameter ε, and look for asymptotic expansion of the solution. Following Ref. [4] and making use of the Weyl calculus [6], the diagonalization of the operator $\hat{\mathsf{D}}$ leads to decoupling of mode polarizations, and to a scalar wave equation for each scalar wave function $\phi^{(\mu)}$ (to be defined below), which is written as

$$\hat{\lambda}^{(\mu)}\phi^{(\mu)}=0, \tag{2}$$

where μ denotes the single mode, and $\hat{\lambda}^{(\mu)}$ is a scalar operator. It is obtained by applying the inverse of the Weyl transform to the eigenvalue $\lambda^{(\mu)}$ of the Weyl symbol $\mathsf{D}(\boldsymbol{x},\boldsymbol{k})$ of the wave operator $\hat{\mathsf{D}}$ (see Appendix). The diagonalization of the matrix $\mathsf{D}(\boldsymbol{x},\boldsymbol{k})$ has to be performed up to first order in ε.

The eigenvalues $\lambda^{(\mu)}$ are

$$\lambda^{(F)}=4\pi\rho\omega^2-k^2B^2 \tag{3}$$

and

$$\lambda^{(A)}=4\pi\rho\omega^2-(\boldsymbol{k}\cdot\boldsymbol{B})^2, \tag{4}$$

where (F) and (A) denote fast and shear Alfvén modes, respectively, and the third mode corresponds here to zero frequency. The relevant polarization vectors [defined in the $(\boldsymbol{x},\boldsymbol{k})$ phase space] can be viewed as the eigenvectors of the Weyl symbol D, and are

$$\boldsymbol{\tau}^{(F)}=\frac{\boldsymbol{B}\times(\boldsymbol{B}\times\boldsymbol{k})}{|\boldsymbol{B}\times(\boldsymbol{B}\times\boldsymbol{k})|}, \tag{5}$$

$$\boldsymbol{\tau}^{(A)}=\frac{\boldsymbol{B}\times\boldsymbol{k}}{|\boldsymbol{B}\times\boldsymbol{k}|}. \tag{6}$$

We note that in this specific case the first order term of λ vanishes since $\hat{\mathsf{D}}$ is symmetric, as has been already pointed out in Ref. [7].

From Eqs. (3) and (4), by means of the Weyl calculus [Eqs. (A4), (A2), and (A1)], we obtain explicitly

$$\hat{\lambda}^{(F)}\phi^{(F)}=4\pi\rho\omega^2\phi^{(F)}+\nabla\cdot(B^2\nabla\phi^{(F)})=0, \tag{7}$$

and

$$\hat{\lambda}^{(A)}\phi^{(A)}=4\pi\rho\omega^2\phi^{(A)}+(\boldsymbol{B}\cdot\nabla)(\boldsymbol{B}\cdot\nabla)\phi^{(A)}=0. \tag{8}$$

The displacement vector $\boldsymbol{\xi}$, solution of Eq. (1), is then related to ϕ, and $\boldsymbol{\tau}$, by the transform

$$\boldsymbol{\xi}(\boldsymbol{x})=\frac{1}{(2\pi\varepsilon)^3}\int d\boldsymbol{x}'d\boldsymbol{k}\phi(\boldsymbol{x}')\boldsymbol{\tau}\left(\frac{\boldsymbol{x}+\boldsymbol{x}'}{2},\boldsymbol{k}\right)\times\exp[i\boldsymbol{k}\cdot(\boldsymbol{x}-\boldsymbol{x}')/\varepsilon], \tag{9}$$

which has to be taken asymptotically to lowest order in ε.

When the WKB ansatz is made to solve the equation for ϕ for each mode,

$$\phi(\boldsymbol{x})=A(\boldsymbol{x})\exp[iS(\boldsymbol{x})/\varepsilon], \tag{10}$$

the eikonal S and the amplitude A can be determined solving the Hamilton-Jacobi equation for S:

$$\lambda(\boldsymbol{x},\boldsymbol{k})=0, \tag{11}$$

and the amplitude transport equation

$$\frac{\partial}{\partial\boldsymbol{x}}\cdot\left(A^2\frac{\partial\lambda}{\partial\boldsymbol{k}}\right)=0, \tag{12}$$

where $\boldsymbol{k}(\boldsymbol{x})=\partial S/\partial\boldsymbol{x}$. Discussions relevant to the solution of this equation can be found, e.g., in Refs. [8,9]. The function $\lambda(\boldsymbol{x},\boldsymbol{k})$ plays the role of the ray Hamiltonian for the scalar field ϕ, and the ray trajectories are given by the Hamilton's equations

$$\dot{\boldsymbol{x}}=\frac{\partial\lambda}{\partial\boldsymbol{k}}, \tag{13a}$$

$$\dot{\boldsymbol{k}}=-\frac{\partial\lambda}{\partial\boldsymbol{x}}. \tag{13b}$$

Evaluation of the integral (9) by the stationary phase method gives

$$\boldsymbol{\xi}(\boldsymbol{x})=\boldsymbol{\tau}(\boldsymbol{x},\boldsymbol{k})A(\boldsymbol{x})\exp[iS(\boldsymbol{x})/\varepsilon]\quad\text{with}\quad\boldsymbol{k}=\partial S/\partial\boldsymbol{x} \tag{14}$$

for each mode. Note that, in general, for each polarization the eigenmodes of the system are made by a proper superposition of integrals of the form (9). Moreover, at the caustics, where the plain WKB expression (14) diverges, a proper treatment of the expression (9) is required.

In the configurations under consideration, λ does not depend on z, and k_z is a constant of motion. Since the system is periodic in z, $k_z=2\pi n/L_z$, where n is integer, and L_z is the z periodicity length.

From the analysis of the ray trajectories, it is easily found that trapping of shear Alfvén waves does not occur. Fast waves can instead be trapped in a region close to the X line, which is a minimum of B^2. In fact, following [8], the ray trajectories can be derived from the Hamiltonian

$$h(\boldsymbol{x},\boldsymbol{k})=\frac{1}{2}k^2-\frac{2\pi\rho\omega^2}{B^2(x,y)}=0, \tag{15}$$

where the term $k^2/2$ has the role of a kinetic energy, and $-2\pi\rho\omega^2/B^2$ of a 2D potential. In the following, we shall consider the fast mode only.

III. THE UNPERTURBED FIELD

The planar field $\boldsymbol{B}_p(x,y)$ can be represented by means of a flux function $\psi(x,y)$,

$$\boldsymbol{B}_p(x,y)=\nabla\psi\times\boldsymbol{e}_z, \tag{16}$$

with $\nabla^2\psi=0$, since $\nabla\times\boldsymbol{B}_p=\boldsymbol{0}$.

Here, we consider two different magnetic configurations. In the first case, the flux function describes a pure hyperbolic magnetic field:

$$\psi=\frac{B_{p0}}{L}(y^2-x^2), \tag{17}$$

where L is a scale length, and B_{p0} a scale poloidal field. The field line projections on the (x,y) plane (i.e., the curves $\psi=$ const) are hyperbolae. The poloidal magnetic field components are $B_x=2B_{p0}y/L$ and $B_y=2B_{p0}x/L$, and B^2 is

$$B^2=B_z^2+4B_{p0}^2\frac{(x^2+y^2)}{L^2}. \tag{18}$$

In the second case, a two-wire configuration is considered, in which $\boldsymbol{B}_p$ is due to two equal currents flowing in two wires parallel to the z axis, located at $y=\pm L$ on the y axis. The corresponding flux function is

$$\psi=-\frac{B_{p0}L}{2}\ln\left[\frac{(x^2-y^2+L^2)^2+4x^2y^2}{L^4}\right], \tag{19}$$

and the magnetic field amplitude is

$$B^2=B_z^2+4B_{p0}^2L^2\frac{x^2+y^2}{(x^2-y^2+L^2)^2+4x^2y^2}. \tag{20}$$

In the limit $x^2+y^2\ll L^2$, i.e., close to the X line, the two-wire configuration approaches the hyperbolic configuration. The contour plots of ψ and B^2 for the two cases are shown in Figs. 1–4. We note the presence of a region of increasing B^2 around the X point.

In the following, dimensionless variables are used (without change of notation), so that length, magnetic field, and

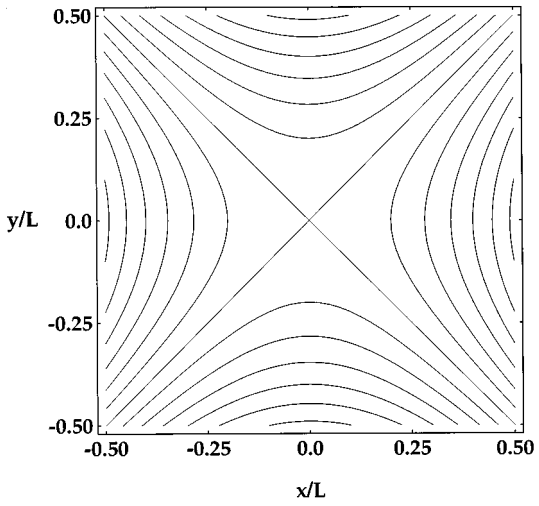

FIG. 1. Contour lines of the flux function ψ defined by Eq. (17), in the neighborhood of the X point, in the (x,y) plane.

time are measured, respectively, in units of L, B_z, and $t_A = L\sqrt{4\pi\rho}/B_z = L/c_A$, c_A being the Alfvén speed in the field B_z.

IV. ANALYSIS OF THE EIGENMODES

In the hyperbolic case, the ray Hamiltonian (3) reads, in cylindrical coordinates (r,ϑ,z),

$$\lambda(r,\vartheta,k_r,k_\vartheta,k_z) = \omega^2 - \left({k_r}^2 + \frac{{k_\vartheta}^2}{r^2} + {k_z}^2 \right)(1+\alpha^2 r^2), \quad (21)$$

where the covariant components k_r, k_ϑ, k_z are the momenta conjugate to r,ϑ,z, $r^2 = x^2 + y^2$, and $\alpha = 2B_{p0}/B_z$.

In this case, the problem is reduced to quadrature, with $k_\vartheta = \text{const} = m$ being an integral of motion, and k_r given by

$${k_r}^2 = \frac{\omega^2}{1+\alpha^2 r^2} - \frac{m^2}{r^2} - {k_z}^2. \quad (22)$$

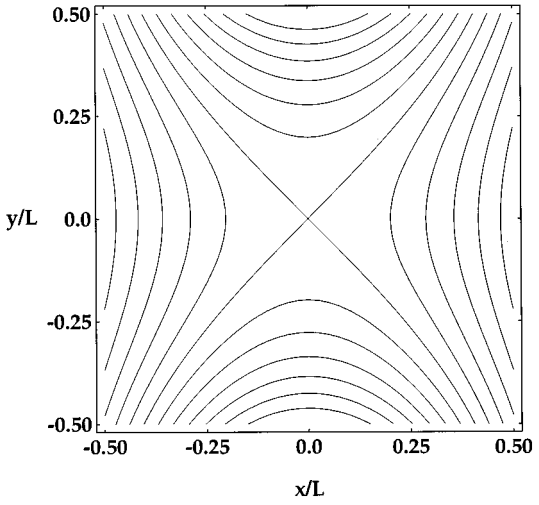

FIG. 2. Contour lines of the flux function ψ defined by Eq. (19), in the neighborhood of the X point, in the (x,y) plane.

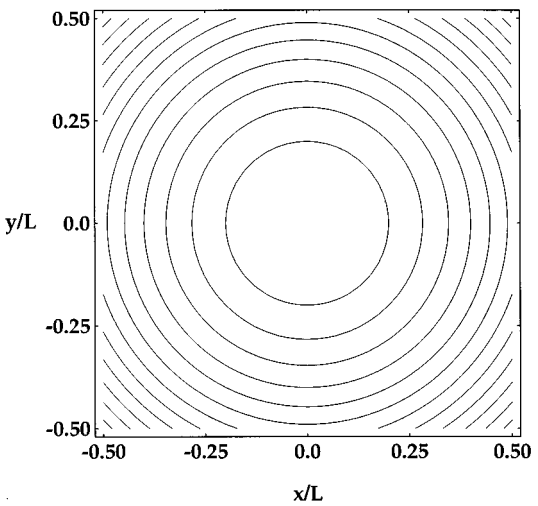

FIG. 3. Contour lines of the magnetic field amplitude given by Eq. (18), in the neighborhood of the X point, in the (x,y) plane.

In the framework of the geometrical optics, wave propagation occurs for $k_r^2 \geqslant 0$. This condition can be met if $\omega^2 \geqslant \omega_{\min}^2 = (\alpha m + k_z)^2$. At any frequency below $\omega_{\min}$, the mode is evanescent, so that this requirement gives a lower bound to the spectrum. The roots of the equation ${k_r}^2(r) = 0$ give the radii of the caustics, which are cylindrical surfaces coaxial to the z axis. In the case $k_z = 0$ (analyzed in Refs. [1,2]), this equation has no solutions for $m = 0$ (axisymmetric modes), and propagation is allowed for any value of r. For $m \neq 0$, there is one solution, corresponding to an internal caustic where reflection of the incoming rays takes place: this caustic limits a region of no propagation around the X point. In the general case $k_z \neq 0$, there are two solutions r_1 and r_2, so that the ray trajectory is trapped in the region $r_1 \leqslant r \leqslant r_2$, inside two caustics. The shape of the accessibility region is determined by the quantum number m. For $m = 0$, the internal caustic disappears ($r_1 = 0$), and the trapping region contains the X point.

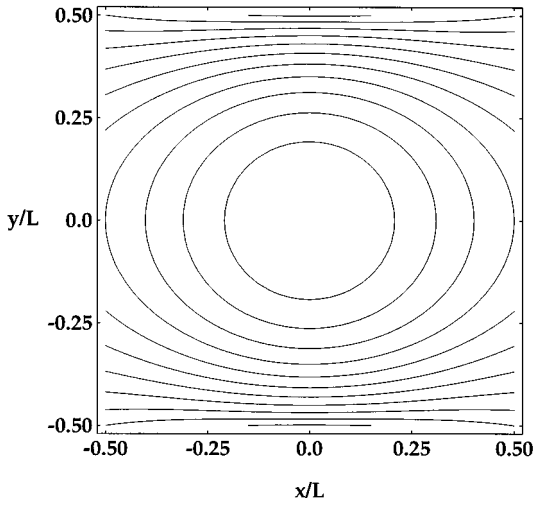

FIG. 4. Contour lines of the magnetic field amplitude given by Eq. (20), in the neighborhood of the X point, in the (x,y) plane.

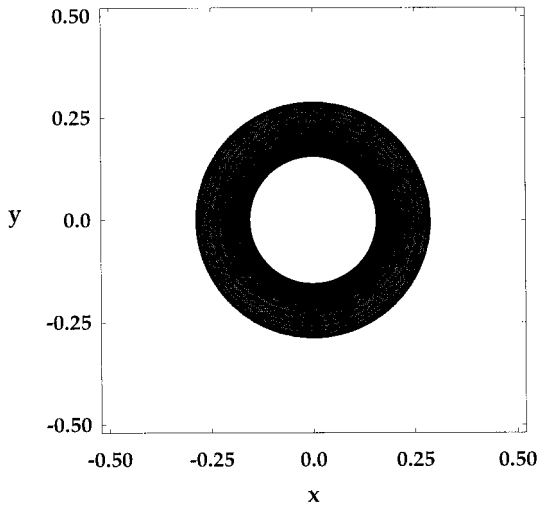

FIG. 5. Example of a ray trajectory projected in the (x,y) plane, for the case of the pure hyperbolic magnetic field. The chosen parameters are $\alpha=1/3$, $L/L_z=1/3$, $n=1000$, $m=5$, and $n_r=0$.

The eigenfrequencies of the system can be obtained from the semiclassical quantization rule for the radial action

$$J_r=J_r(\omega,n,m)\equiv\frac{1}{\pi}\int_{r_1}^{r_2}k_r dr=n_r+\frac{1}{2}, \tag{23}$$

where n_r is the radial quantum number. The eigenvalue spectrum $\omega^2(n_r,m,n)$ is given implicitly by Eq. (23). For the parabolic profile of B^2 under consideration, J_r can be expressed by means of elliptic integrals, and the spectrum can be evaluated numerically. No degeneracy is foreseen in Eq. (23).

An example of a single, ''rose''-shaped, ray trajectory, projected in the (x,y) plane, is shown in Fig. 5. As discussed above, wave propagation occurs in a well-defined region delimited by two caustics defined by $r_1\leqslant r\leqslant r_2$, and the region containing the X line is not accessible to the wave.

The WKB eigenfunctions are given by a proper superposition of terms (10). From Eqs. (11) and (12), we obtain for the eikonal function S, and the amplitude A, $S(r,\vartheta,z)=\int^r k_r dr+m\vartheta+k_z z$, and $rk_rB^2A^2=$ const, with k_r given by Eq. (22). The solution, diverging at the caustics, then can be made continuous by standard techniques. The solution thus obtained is a very good approximation of the solution of the wave equation (7), which, putting $\varphi=\tilde{\varphi}(r)\exp(im\vartheta+ik_z z)$, is written as (in dimensionless variables)

$$\frac{1}{r}\frac{\partial}{\partial r}\left(rB^2\frac{\partial\tilde{\varphi}}{\partial r}\right)+\left[\omega^2-B^2\left(\frac{m^2}{r^2}-k_z^2\right)\right]\tilde{\varphi}=0. \tag{24}$$

A representation of the eigenfunction $\tilde{\varphi}(r)\exp(im\vartheta)$ is shown in Fig. 6 for the same parameters as in Fig. 5.

A fully analytical treatment can be performed in the limit of wave propagation mostly along the z axis, and weak poloidal field, i.e., for $k_z^2\gg k_\perp^2=k_r^2+m^2/r^2$, and $\alpha^2r^2\ll1$. In this case, the Hamiltonian (21) can be approximated by means of the following Hamiltonian, where the term $k_\perp^2B_p^2$ has been dropped:

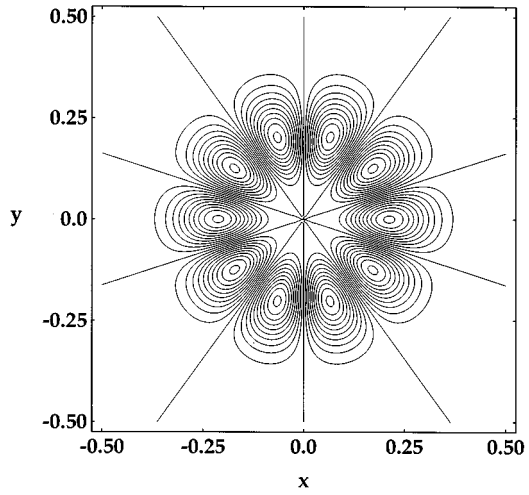

FIG. 6. Plot of the eigenfunction $\tilde{\varphi}(r)\cos(m\vartheta)$, solution of Eq. (24), for the same parameters as in Fig. 5.

$$\lambda(r,k_r,k_\vartheta,k_z)=\omega^2-\left(k_r^2+\frac{k_\vartheta^2}{r^2}+k_z^2B^2\right). \tag{25}$$

The above Hamiltonian can be formally referred to the 1D motion of a particle with kinetic energy $2k_r^2$ in the effective potential $V(r)=k_\vartheta^2/r^2+k_z^2B^2$. The corresponding wave equation (obtained inverting the Weyl symbol) is

$$\frac{1}{r}\frac{\partial}{\partial r}\left(r\frac{\partial\tilde{\varphi}}{\partial r}\right)+\left[\omega^2-\frac{m^2}{r^2}-k_z^2(1+\alpha^2r^2)\right]\tilde{\varphi}=0. \tag{26}$$

This equation is a Schrödinger equation in the effective potential $V(r)$, and has the solution $\tilde{\varphi}=r^{|m|}\exp(-\alpha k_z r^2/2)L_{n_r}^{|m|}(\alpha k_z r^2)$, $L_{n_r}^{|m|}$ being the generalized Laguerre polynomial. The quantum number n_r is related to ω by the equation

$$\omega^2(n_r,m,n)=k_z{}^2+2\alpha k_z(2n_r+|m|+1). \tag{27}$$

Equation (27) gives the eigenfrequencies explicitly in terms of the quantum number set (n_r,m,n), and coincides exactly with the WKB spectrum obtained by applying the quantization rule (23) to the Hamiltonian (25), since the potential is that of a (cylindrical) harmonic oscillator. In this case, the spectrum is degenerate, and the angular precession is lost. Equation (26) can be directly obtained from Eq. (24) by simply dropping the term $\nabla_\perp\cdot(\alpha^2r^2\nabla_\perp\tilde{\varphi})\equiv\alpha^2[1/r\partial/\partial r(r^3\partial\tilde{\varphi}/\partial r)-m^2\tilde{\varphi}]$. The contribution of this term to the eigenfrequency can be easily computed by means of perturbation theory [10]. Normalizing the radial coordinate r over $\sqrt{\alpha k_z}$, the perturbation parameter is identified as α/k_z. The frequency spectrum, up to first order in α/k_z, is

$$\omega^2(n_r,m,n)=k_z{}^2+2\alpha k_z(2n_r+|m|+1)+\alpha^2(2n_r^2+2n_r+2+m^2+2n_r|m|+|m|). \tag{28}$$

Note that the degeneracy in Eq. (27) is now removed.

In the case of the two-wire magnetic configuration, described by Eqs. (19) and (20), trapping of the fast wave in

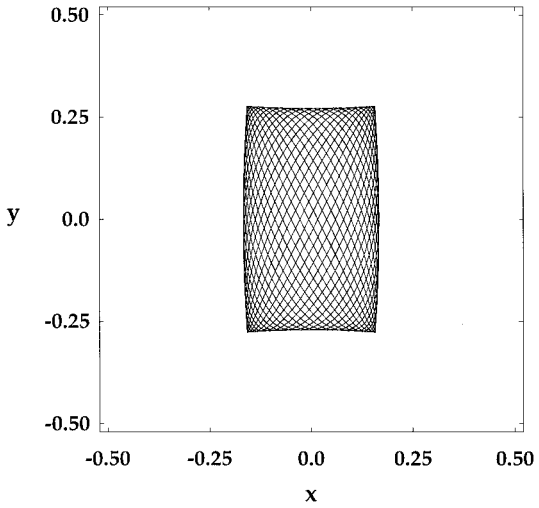

FIG. 7. Example of a ray trajectory projected in the (x,y) plane, for the case of the two-wire configuration. The chosen parameters are very close to those in Fig. 5.

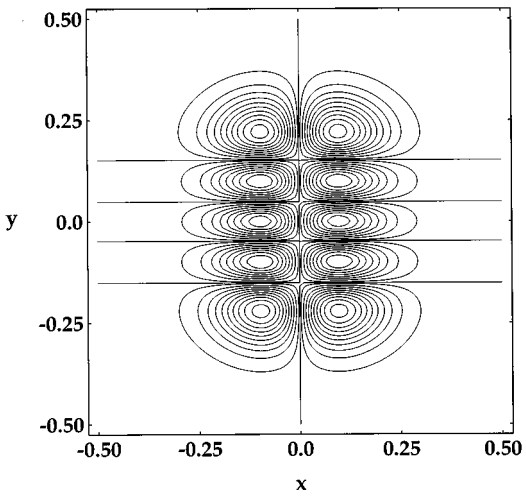

FIG. 8. Plot of the eigenfunction $\tilde{\varphi}(x,y)$, solution of Eq. (34), for $n_x=1$, $n_y=4$, and $n=1000$. The corresponding trajectory is that shown in Fig. 7.

the region around the X point can occur for large enough k_z. For low values of k_z, only traveling waves are found. The pattern of the trapped ray trajectories is considerably different from that predicted in the asymptotic limit, as can be seen in Fig. 7, where a ray trajectory is represented for parameters very close to those of Fig. 5. Now, only one caustic is still present, and the region containing the X line is accessible to the wave. Since the magnetic field amplitude (20) depends on both the canonical coordinates r and ϑ, k_ϑ is no longer a constant of motion. Its variation allows the wave to propagate into the region around $r=0$.

To exploit the observed differences of the ray topology in the two magnetic configurations, we consider the following Hamiltonian, obtained by taking into account terms of order $O(r^4)$ in the series expansion of the magnetic field amplitude (20) around the X point:

$$\lambda(r,\vartheta,k_r,k_\vartheta,k_z)=\omega^2-\left(k_z{}^2+k_r{}^2+\frac{k_\vartheta{}^2}{r^2}\right)\times(1+\alpha^2r^2-2\alpha^2r^4\cos 2\vartheta). \quad (29)$$

The ray trajectories obtained from this Hamiltonian show the same topology as those computed by inserting in the Hamiltonian the exact magnetic field (20), as far as they are confined in the region close to the X point.

In the same limit performed previously, (i.e., $k_z^2\gg k_\perp^2=k_x^2+k_y^2$ [see Eq. (25)]), the Hamiltonian (29) is separable when expressed in Cartesian canonical coordinates (x,k_x,y,k_y), and corresponds to two uncoupled nonlinear oscillators:

$$\begin{aligned}\lambda(x,y,k_x,k_y,k_z)&=\omega^2-k_z^2-[H_x(x,k_x)+H_y(y,k_y)]\\&=\omega^2-k_z^2-[k_x^2+\alpha^2k_z^2(x^2-2x^4)+k_y^2\\&\quad+\alpha^2k_z^2(y^2+2y^4)].\end{aligned} \quad (30)$$

In this approximation, the problem is reduced to quadrature, i.e., $H_x(x,k_x)=H_x$, and $H_y(y,k_y)=H_y$, where H_x and H_y are two constants satisfying $\overline{H_x}+\overline{H_y}=\omega^2-k_z^2$. The ray dynamics is given by the superposition of two independent 1D periodic motions (with different frequencies) between the turning points $x^{(\pm)}=\pm|\overline{x}|$, and $y^{(\pm)}=\pm|\overline{y}|$, which are the roots of the equations

$$\begin{aligned}k_x^2&=\overline{H_x}-\alpha^2k_z^2(x^2-2x^4)=0,\\k_y^2&=\overline{H_y}-\alpha^2k_z^2(y^2+2y^4)=0.\end{aligned} \quad (31)$$

The resulting caustic in the (x,y) plane is a rectangle of sides $2|\overline{x}|$ and $2|\overline{y}|$ centered in the origin, and with sides parallel to the coordinate axes.

The frequency spectrum can be found by applying the semiclassical quantization rule to each oscillator separately:

$$\begin{aligned}J_x&=J_x(\overline{H_x},n)\equiv\frac{2}{\pi}\int_0^{\overline{x}}k_x dx=n_x+\frac{1}{2},\\J_y&=J_y(\overline{H_y},n)\equiv\frac{2}{\pi}\int_0^{\overline{y}}k_y dy=n_y+\frac{1}{2},\end{aligned} \quad (32)$$

where the action integrals J_x and J_y can be expressed in terms of elliptic integrals. In the relevant limit $n\gg n_x,n_y$, an approximate explicit form of Eq. (32) can be found:

$$\omega^2(n,n_x,n_y)=k_z^2+2\alpha k_z(n_x+n_y+1)-3[(n_x+\tfrac{1}{2})^2-(n_y+\tfrac{1}{2})^2]. \quad (33)$$

The parameter characterizing the deviation with respect to cylindrical symmetry of the magnetic field amplitude can be found by normalizing the spatial variables, x and y, over $\sqrt{\alpha k_z}$. In this case, one obtains $(\alpha k_z)^{-1}$. The expression (33) can be obtained also by means of the perturbation theory applied to the Hamiltonian (30), at first order in the smallness parameter $(\alpha k_z)^{-1}$. Comparing Eq. (33) with Eq. (27), it is found that the breaking of axial symmetry introduces an additional term, which removes the degeneracy in the eigen-

frequencies. The eigenfrequencies (33) merge into the eigenfrequencies (27) in the limit $(\alpha k_z)^{-1} \to 0$ (with the correspondence $2n_r + |m| = n_x + n_y$). This can be understood since the linear size of the caustic scales as $(\alpha k_z)^{-1}$.

In the considered limit, the wave equation (7) is written as

$$\left(\frac{\partial^2}{\partial x^2} + \frac{\partial^2}{\partial y^2} \right) \tilde{\varphi}(x,y) + [\omega^2 - k_z^2 - \alpha^2 k_z^2 (x^2 - 2x^4 + y^2 + 2y^4)] \tilde{\varphi}(x,y) = 0, \quad (34)$$

with $\varphi = \tilde{\varphi}(x,y) \exp(ik_z z)$. The above equation can be solved by separation of variables. The solution corresponding to the case plotted in Fig. 7 is shown in Fig. 8. Note that the structure of the eigenfunction is different from that found in the hyperbolic configuration.

V. CONCLUSIONS

We have investigated the frequency spectrum, and the corresponding eigenfunctions relevant to fast waves trapped around a X line, and have explicitly considered the hyperbolic configuration of the magnetic field and the two-wire configuration. We observe that, for a given eigenfrequency, an eigenfunction of the system characterizes in a unique way the structure of the mode only when degeneracy is absent. This actually occurs in the case of the pure hyperbolic configuration, and of the two-wire configuration. The eigenfunctions relevant to the two different magnetic configurations have a quite different structure even in a region close to the X point.

We then conclude that the structure of the fast waves trapped around a X line is very sensitive to the actual magnetic configuration. Even arbitrary small perturbations of the magnetic field, which break the symmetry of the pure hyperbolic configuration, can strongly modify the wave pattern.

ACKNOWLEDGMENT

We thank Allan Kaufman for useful discussions.

APPENDIX

We recall here, following Refs. [4,6], the definitions of the Weyl symbol used in the text. Let us consider the equation

$$\hat{\mathsf{A}} \boldsymbol{\psi} = \mathbf{0}, \quad (A1)$$

where the operator $\hat{\mathsf{A}}$ is Hermitian. Using the configuration space representation, this equation can be written in the form

$$\int d\boldsymbol{x}' \, \mathcal{A}(\boldsymbol{x}, \boldsymbol{x}') \boldsymbol{\psi}(\boldsymbol{x}') = \mathbf{0}, \quad (A2)$$

where $\mathcal{A}$ is the kernel.

The Weyl symbol of the operator $\hat{\mathsf{A}}$ is defined as

$$\mathsf{A}(\boldsymbol{x}, \boldsymbol{k}) = \int d\boldsymbol{s} \mathcal{A}\left(\boldsymbol{x} + \frac{\boldsymbol{s}}{2}, \boldsymbol{x} - \frac{\boldsymbol{s}}{2} \right) \exp[-i\boldsymbol{k} \cdot \boldsymbol{s}/\varepsilon]. \quad (A3)$$

The inverse of the Weyl symbol is defined as

$$\mathcal{A}(\boldsymbol{x}, \boldsymbol{x}') = \frac{1}{(2\pi\varepsilon)^3} \int d\boldsymbol{x}' \mathsf{A}\left(\frac{\boldsymbol{x} + \boldsymbol{x}'}{2}, \boldsymbol{k} \right) \exp[i\boldsymbol{k} \cdot (\boldsymbol{x} - \boldsymbol{x}')/\varepsilon]. \quad (A4)$$

[1] S. V. Bulanov and S. I. Syrovatskii, Fiz. Plazmy **6**, 1205 (1980) [Sov. J. Plasma Phys. **6**, 661 (1980)].
[2] S. V. Bulanov, F. Pegoraro, and S. G. Sasharina, Plasma Phys. Controlled Fusion **32**, 377 (1990); S. V. Bulanov, S. G. Sasharina, and F. Pegoraro, Plasma Phys. Controlled Fusion **34**, 33 (1992); S. V. Bulanov and F. Pegoraro, Plasma Phys. Rep. **19**, 585 (1993).
[3] I. M. Rutkevich and M. Mond, Phys. Plasmas **1**, 3792 (1994).
[4] R. G. Littlejohn and W. G. Flynn, Phys. Rev. A **44**, 5239 (1991).
[5] L. Friedland and A. N. Kaufman, Phys. Fluids **30**, 3050 (1987).
[6] S. W. MacDonald, Phys. Rep. **158**, 339 (1988).
[7] H. L. Berk and D. Pfirsch, J. Math. Phys. **21**, 2054 (1980).
[8] S. Weinberg, Phys. Rev. **126**, 1899 (1962).
[9] R. G. Littlejohn, J. Stat. Phys. **68**, 7 (1992).
[10] L. D. Landau and E. M. Lifshitz, *Quantum Mechanics. Non-relativistic Theory* (Pergamon Press, Oxford, 1965).